Mon. Not. R. Astron. Soc. (1992) **259**, Short Communication, 5P–7P

Infrared observations of the gravitational lens system B1422 + 231

C. R. Lawrence,[1] G. Neugebauer,[1] N. Weir,[1] K. Matthews[1] and A. R. Patnaik[2]

[1] *Palomar Observatory, California Institute of Technology, Pasadena, CA 91125, USA*

[2] *University of Manchester, Nuffield Radio Astronomy Laboratories, Jodrell Bank, Macclesfield, Cheshire SK11 9DL*

Accepted 1992 August 26. Received 1992 August 21

ABSTRACT

Images of the multiple-component radio source B1422+231 at 2.2 μm show the structure of this source to be essentially the same at radio and infrared frquencies. The most natural explanation for this achromatic structure is gravitational lensing.

Key words: gravitational lensing – infrared: galaxies – radio continuum: galaxies.

1 INTRODUCTION

The radio source B1422+231, at $z = 3.62$, comprises four components with a maximum separation of 1.3 arcsec (see companion paper by Patnaik et al., this issue). As named by Patnaik et al., A, C and D form an almost equilateral triangle, with B 0.5 arcsec from A near the AC side. The components are unresolved in a MERLIN 5-GHz image with 50-mas resolution. As discussed by Patnaik et al., the similarity of the radio spectral indices, polarization and polarization angle of the brightest three components all suggest gravitational lensing as the origin of the highly unusual structure of B1422+231.

Since gravitational lensing itself is achromatic, multiple images must have approximately the same structure and relative amplitudes at all frequencies. This is rarely or never seen between multiple components of unlensed sources. For this reason, optical imaging is the normal second step in radio searches for gravitational lenses (e.g. Lawrence et al. 1984). Infrared imaging offers the important advantage over optical imaging of better seeing, and in this paper we describe our infrared observations of B1422+231.

2 OBSERVATIONS AND ANALYSIS

B1422+231 was observed on 1992 March 13 with the Caltech 58 × 62 InSb array camera at the Cassegrain focus of the Hale telescope. The pixel size is 0.314 arcsec. A series of eight exposures was made in the 2.0–2.4 μm K band, with a total integration time of 480 s. To facilitate removal of the sky background, the B1422+231 system was placed in several different locations on the array, and the telescope tracking was controlled by an offset autoguider. The seeing was excellent (FWHM ≈ 0.5 arcsec), although changing telescope focus following a drop in air temperature led to a steady increase in image size during the observations. That and astigmatism in the 200-inch mirror gave unresolved images of ~ 0.75 arcsec (FWHM).

Individual images were flattened and corrected for non-linearity. The sky level subtracted from each image was from an adjacent image in the series containing no sources in the region near B1422+231. Fig. 1(a) (opposite page 6P) shows one of the individual K-band images after flattening and sky subtraction. To the resolution and sensitivity limit of the infrared images, the correspondence between infrared and radio emission is excellent, providing strong evidence that B1422+231 is gravitationally lensed.

Although the scatter in the total brightness of the eight images was only 0.03 mag, conditions were not photometric. Calibration based on a standard star observation from the previous (photometric) night thus gives an upper limit of $K = 12.7$ mag for the total B1422+231 system.

The individual images were combined for maximum sensitivity. Since the pixels of the array are relatively large, the images were rebinned to 0.0314-arcsec pixels, shifted by integral (small) pixels according to the relative guider offsets, and averaged. The result is shown in Fig. 1(b) (opposite page 6P).

Fig. 1(b) clearly shows emission south-east of AB and east of C, but also has lower resolution than the individual images. To see if the infrared emission was consistent with three unresolved counterparts of radio components A, B and C, Gaussians were fitted to the individual K-band images as follows. (i) A single elliptical Gaussian was fitted to 'A+B'. (ii) With all parameters of the A+B Gaussian fixed, a second Gaussian was fitted to the south-western peak 'C'. Since that peak is somewhat separated from the rest of the emission, it provides the best available means of determining the point spread function (PSF) in the images. (iii) The width and orientation of the C Gaussian were fixed, and two Gaussians with the same fixed width and orientation were fitted to A+B. This final step gives the positions and amplitudes of three unresolved components that best represent the emission.

The mean values of these positions and amplitudes for the eight K images are given in Table 1. The maximum discrep-

Table 1. Relative positions and photometry.

	Radio[a]			Avg. Infrared[b]			MEM Infrared[c]		
COMPONENT	$\Delta\alpha$	$\Delta\delta$	Ampl.	$\Delta\alpha$	$\Delta\delta$	Ampl.	$\Delta\alpha$	$\Delta\delta$	Ampl.
A	0″.39	0″.32	0.977	0″.30	0″.42	0.84	0″.31	0″.37	0.78
B	0.00	0.00	1.000	0.00	0.00	1.00	0.00	0.00	1.00
C	−0.33	−0.75	0.520	−0.33	−0.68	0.51	−0.34	−0.71	0.49
D	0.94	−0.81	0.020	...	...	<0.034	0.96	−0.71	0.06

[a]MERLIN 5 GHz, from Patnaik et al. Radio position uncertainties are < 0.01 arcsec. [b]Mean relative positions and amplitudes of Gaussians fitted to A, B and C in each of the eight individual *K*-band images, as described in the text. D was too faint to be fitted in the individual images. The upper limit on its relative amplitude was determined by aperture photometry in the combined image (middle panel of Fig. 1), as described in the text. Statistical uncertainties in relative positions are ~0.03 arcsec, based on scatter among the eight individual images; however, undersampling of the images, coupled with component separations of a few pixels or less, undoubtedly leads to significant systematic errors. [c]Relative positions are calculated between centroids, and amplitudes are integrated signal in circular apertures.

ancy between radio and infrared relative positions is 0.14 arcsec or 0.4 pixels, and the maximum discrepancy in relative amplitudes is 14 per cent. It is difficult to estimate the errors introduced by undersampling; however, given that for both position and amplitude the largest discrepancy occurs for the closest components, we conclude that the relative positions and amplitudes of A, B and C are the same in the radio and the infrared to within the errors.

The ratio of the signal in a small circular aperture centred on the position of D to the total signal for the entire system is 0.014. Since the wings of A, B and C extend into the aperture, this is an upper limit to unresolved flux coincident with D. This gives D/B ≤3.4 per cent.

To make maximum use of spatial information in the original images, a maximum entropy method (MEM) deconvolution was attempted, using the procedure described in Weir (1991, 1992). The procedure took as input: (i) 16 × 16 subsets of the eight original images (0.314-arcsec pixels), centred to the nearest pixel on C; (ii) the position in each subset image of the Gaussian fit to C; (iii) rms noise levels in each image; and (iv) 128 × 128 pixel PSF estimates for each image using 0.0628-arcsec pixels. The PSFs were approximated as 2D Gaussians of unit amplitude, whose widths and orientations were those of the Gaussian fits to C in each image. A multichannel MEM model was applied (see Weir 1992), which explicitly incorporates a preference for smoothness in the reconstruction. This suppresses the tendency of traditional MEM implementations to deconvolve extended regions into numerous spurious point sources.

Fig. 1(c) (opposite page 6P) shows the result, and Table 1 gives relative positions and amplitudes. Positional agreement with the radio image is excellent. The MEM offsets from B of A, C and D differ from the radio offsets by 0.09, 0.04 and 0.10 arcsec, respectively, less than one-third of an array pixel. (The *separation* AB of 0.48 arcsec agrees extremely well with the radio separation of 0.50 arcsec.) Once again, the largest disagreements are for the closest pair and the faintest component. We see no reason to doubt that unresolved counterparts to all four radio components of B1422 + 231 have been detected. Since MEM reconstructions are photometrically unreliable, especially for faint objects, we trust the upper limit on D, obtained from the combined image, more than the MEM value.

The MEM image contains several emission peaks other than A, B, C and D. The strongest of these is 0.16 arcsec east and 0.64 arcsec north of A, with an amplitude 75 per cent that of D. Patnaik et al. report no radio emission at this location, neither is there obvious emission above the noise level in the combined image (Fig. 1b). Comparisons of MEM images of various subsets of the data, as well as the characteristic separation of the peaks and their spatial arrangement, strongly suggest that they are artefacts of the MEM deconvolution. Errors in the Gaussian approximation to the true PSF and noise in the original images (especially some periodic noise in the readout electronics) might contribute to such errors in reconstruction.

We thus see no reason to believe that these other peaks in the MEM image are real. Conversely, since D can be seen clearly in the combined image, there is no reason to doubt that it *is* real.

3 DISCUSSION

The similarity of the radio and the infrared structure of B1422 + 231 is strong evidence that the four components are gravitational images of the same source. The relative fluxes of the components in Table 1 differ somewhat in the radio and the infrared; however, the largest disagreements are for the closest pair and the faintest component. Given the problems of undersampling and the faintness of D, we are unwilling to conclude that the radio and infrared flux ratios differ significantly. Moreover, the overall spectra of A and D are still much more similar to those of B and C than is ever seen for non-nuclear components of quasars, or the components of compact double radio sources. We thus think it highly likely that all four components are images of a single source, and highly unlikely that two of the radio components might be intrinsic compact double radio structure.

B1422 + 231 is one of the brightest, smallest and highest redshift lens systems known. The most probable redshift for

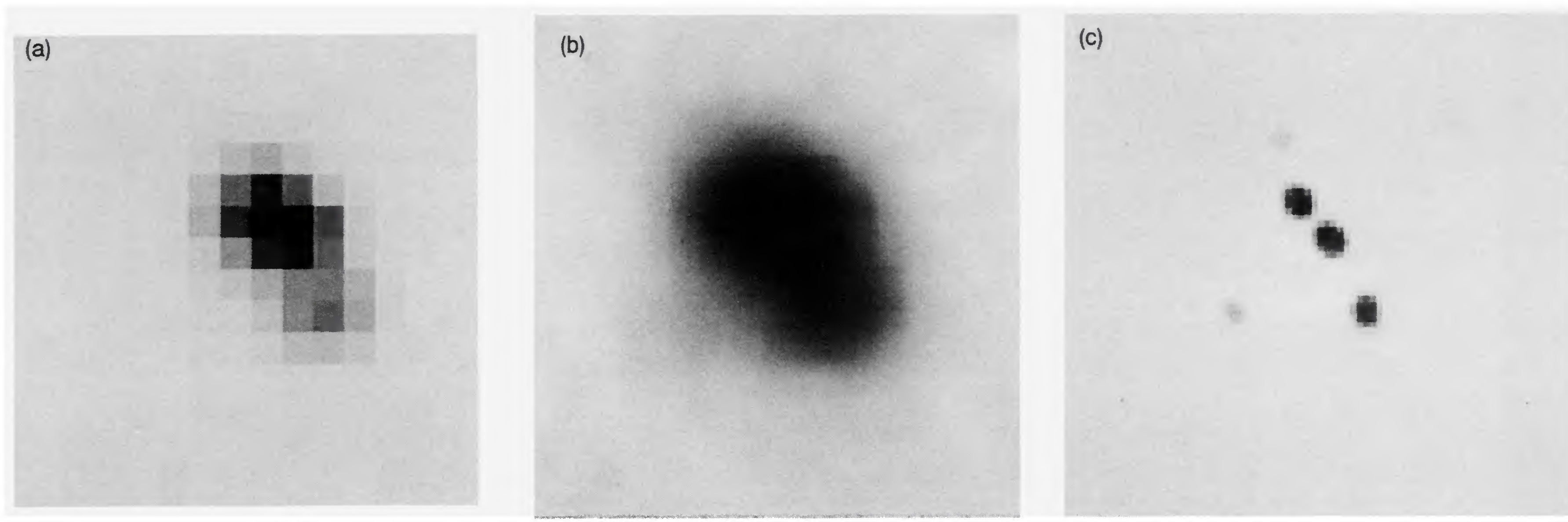

Figure 1. (a) One of eight 60-s K-band images of B1422 + 231. Pixels are 0.314 arcsec square. North is at the top, east is to the left. (b) Image of B1422 + 231 obtained by combining eight 60-s exposures as described in the text. Pixels in this composite are 0.0314 arcsec square. (c) Maximum entropy method reconstruction as described in the text. Pixels are 0.0628 arcsec square.

the lens is $z \sim 1$ (e.g. Kochanek 1992) and, because the splitting is small, the mass and therefore luminosity of the lensing galaxy are unlikely to be large. As even extremely luminous galaxies at $z = 1$ would be difficult to see in the glare of B1422+231, our non-detection of the lens is not surprising. Given the small separation and brightness of the components in B1422+231, detection and measurement of the redshift of the lens will not be easy.

ACKNOWLEDGMENTS

We thank the Palomar staff and night assistant Juan Carrasco for their help with these observations. Infrared and radio astronomy at Caltech are supported by grants from the National Science Foundation.

REFERENCES

Kochanek C. S., 1992, ApJ, 384, 1
Lawrence C. R., Schneider D. P., Schmidt M., Bennett C. L., Hewitt J. N., Burke B. F., Turner E. L., Gunn J. E., 1984, Sci, 223, 46
Patnaik A. R., Browne I. W. A., Walsh D., Chaffee F. H., Foltz C. B, 1992, MNRAS, 259, 1P (this issue)
Weir N., 1991, in Grosbol P. J., Warmels R. H., eds, Proc. 3rd ESO/ST-ECF Data Analysis Workshop. ESO, Garching, p. 115
Weir N., 1992, J. Opt. Soc. Am., submitted